8λ×462Gb/s Transmission with Symmetric Carrier-Assisted Differential Detection Using Delay-Unknown Field Recovery

Yixiao Zhu[1,*], Xiansong Fang[2], Guangying Yang[1], Qunbi Zhuge[1], Weisheng Hu[1], Fan Zhang[2,*]
[1]*State Key Laboratory of Advanced Optical Communication System and Networks, Shanghai Jiao Tong University, Shanghai, 200240, China*
[2]*State Key Laboratory of Advanced Optical Communication System and Networks, Peking University, Beijing, 100871, China*
**Corresponding authors: yixiaozhu@sjtu.edu.cn, fzhang@pku.edu.cn*

Abstract: We implement symmetric carrier-assisted differential detection receiver as an LO-free alternative to single-polarization coherent receiver. Using 2×1 MIMO equalizer-based optical field recovery and SSBI cancellation, 3.7Tb/s(=8λ×462Gb/s) PS-64-QAM signals are transmitted over 25-km SSMF for data-center-interconnects.

1. Introduction

Coherent optics are sinking from long-haul to short-reach scenarios with a typical distance below 80 km [1], owing to its spectrally efficient encoding on both phase- and polarization-diversity, and the field recovery-enabled fiber impairment compensation [2]. However, uncooled lasers are preferred by the cost-sensitive feature of data-center-interconnects (DCI), whose drifting wavelengths impose challenges on colored coherent detection [3]. In this regard, direct detection is inherently colorless and thus can be considered a local oscillator (LO)-free low-cost candidate.

Traditional direct detection receiver has insufficient electrical spectral efficiency (E-SE) with one-dimensional encoding and fiber dispersion-induced power fading obstacle [4], both of which are fundamentally caused by the square-law detection of the photodiode (PD). In recent years, a variety of advanced direct detection schemes have been proposed to improve the SE and achieve optical field recovery [5-10]. Based on the Hilbert transform relationship between the intensity and phase, single-sideband modulation with Kramers-Kronig receiver (KKR) in Fig. 1(a) can accurately reconstruct the complex optical field once the minimum phase condition is satisfied [5]. Nevertheless, taking single-polarization coherent detection as a reference, the data rate and E-SE of KKR is halved because one of the sidebands is wasted. To fill the gap, carrier-less phase retrieval (PR) receiver [6] in Fig.1(b) and carrier-assisted differential detection (CADD) receiver [7] in Fig. 1(c) are designed respectively. In comparison, the CADD receiver can directly reconstruct the optical field from the linear signal-carrier beating, whereas PR receiver extracts from the 2nd-order signal-signal beat interference (SSBI) by using an iterative modified Gerchberg-Saxton (MGS) algorithm [11]. However, the CADD receiver has two remaining issues: 1) it uses an additional single-ended PD branch that are not compatible with standard intradyne coherent receiver design; 2) the transfer function-based field recovery requires precise skew value on the delayed branch.

In this work, we implement a symmetric carrier-assisted differential detection (S-CADD) receiver as a local-oscillator (LO)-free alternative to the single-polarization coherent receiver. Aided by 2×1 multi-input-multi-output (MIMO) equalizer-based optical field recovery and Volterra kernels-based SSBI cancellation (SSBI-C), we experimentally transmit 8-channel wavelength-division-multiplexed (WDM) 462-Gb/s probabilistic-shaped 64-ary quadrature amplitude modulation (PS-64-QAM) signals over 25-km standard single-mode fiber (SSMF). The aggregate capacity is 3.70 Tb/s with a net electrical spectral efficiency of 8.3 b/s/Hz excluding the forward error correction (FEC) overhead, offering a potential candidate for next-generation 3.2T-class DCI campus applications.

2. Principle of symmetric CADD receiver and skew-unknown optical field recovery

The structure of the symmetric CADD receiver is shown in Fig. 1(d). The optical carrier and the information-bearing complex-valued double-sideband signal are C and $s(t)$, respectively. After optical-to-electrical conversion, the output photocurrents I_1 and I_2 of the two balanced photodiodes (BPD) are derived as

$$I_1 = \eta\,\mathrm{Re}\left\{\left(C+s(t-\tau)\right)^*\left(C+s(t)\right)\right\}\Big/2 \tag{1}$$

$$I_2 = \eta\,\mathrm{Im}\left\{\left(C+s(t-\tau)\right)^*\left(C+s(t)\right)\right\}\Big/2 \tag{2}$$

where η is the responsivity of BPD and the factor 1/2 accounts for the splitting ratio of the 90° optical hybrid. After linear combination, the complex-valued waveform $R(t)$ can be obtained as

$$R(t) = I_1 + jI_2 = \eta\left[|C|^2 + Cs^*(t-\tau) + C^*s(t) + s^*(t-\tau)s(t)\right]\Big/2 \tag{3}$$

Given the delay value τ, traditional field recovery is conducted based on the frequency-domain transfer function as

$$s(t) = IFFT\left\{FFT\left\{2\left[R(t)-R^*(t-\tau)\right]-SSBI\right\}\Big/\left(1-e^{-j2\pi f\cdot 2\tau}\right)\right\}\Big/C^* \tag{4}$$

As the reconstruction performance highly relies on the accuracy of τ, we suggest a delay-unknown field recovery algorithm. According to Eq. (3), the 3rd-term is the desired linear signal replica, while the 2nd-term can be regarded as a conjugated inter-symbol interference (ISI) and the 4th-term is the nonlinear SSBI impairment. Based on the observation, we can simply adopt a 2×1 linear MIMO equalizer to eliminate the 2nd-term. Note that 1×1 single-input-single-output (SISO) in Fig. 1(e) cannot address the conjugation term. Fortunately, both real-valued 2×1 MIMO with in-phase and quadrature components or complex-valued form with conjugation components in Fig. 1(f) and 1(g) are feasible. Moreover, the SSBI can be simultaneously mitigated by introducing 2nd-order Volterra kernels.

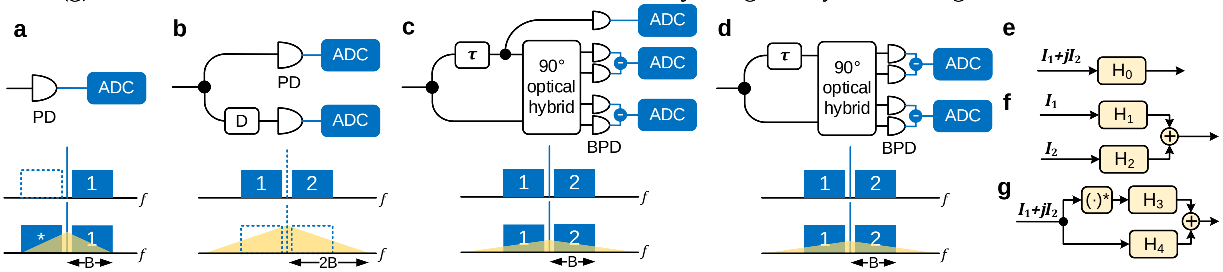

Fig. 1. Receiver structures and optical/electrical signal spectra of (a) Kramers-Kronig receiver, (b) carrier-less phase retrieval receiver, (c) carrier-assisted differential detection receiver, (d) symmetric CADD receiver. D: dispersion element; τ: delay element. Structures of (e) 1×1 SISO, (f) real-valued 2×1 MIMO, (g) complex-valued 2×1 MIMO equalizers.

3. Experimental setup and DSP

The experimental setup of 8-channel WDM transmission with the LO-free symmetric CADD receiver is shown in Fig. 2(a). At the transmitter, an external cavity laser (ECL) at 1550 nm is employed as an optical source, which has 15.4-dBm optical power and 100-kHz linewidth. For the channel under test (CUT), we choose the split-and-combine structure to generate a carrier-assisted complex-valued double-sideband signal. A 27-GHz 3-dB bandwidth IQ modulator (EOspace) is biased at the null point to maximize the linear region, and the carrier-to-signal power ratio (CSPR) is adjusted by the variable optical attenuator (VOA). The two subcarriers (2×42 GBd) electrical signal is generated by a 120-GSa/s arbitrary waveform generator (AWG, Keysight M8194) and amplified by a pair of 50-GHz electrical amplifiers (EA, SHF). For the loading channels, 7 ECLs are spaced at 110 GHz. The IQ modulator 2 is biased above the null point to introduce the same CSPR for emulation. The CUT and loading channels are respectively amplified by polarization-maintaining erbium-doped fiber amplifiers (PM-EDFA) and combined through a wave-shaper. After 25-km SSMF transmission, we use an optical band-pass filter (OBPF) to select the target wavelength channel, which is subsequently amplified by an EDFA to compensate for the loss. Before the symmetric CADD receiver, we place a polarization controller (PC) to align the state of polarization with the 90° optical hybrid, which can be skipped in principle if a dual-polarization hybrid is used. A variable optical delay line is employed in the upper branch to optimize the delay value that is unknown to the receiver-side digital signal processing (DSP). After 70-GHz BPD detection and 50-GHz EA amplification, the electrical waveform is captured by a 256-GSa/s real-time oscilloscope (RTO, Keysight UXR0594AP) for offline DSP. The measured optical spectra of the 8-channel WDM signal at the output port of the wave-shaper is shown in Fig. 2(b). The resolution is 0.01 nm.

Fig. 2(c) and 2(d) shows transmitter- and receiver-side DSP stacks. At the transmitter, the data is mapped to 40960 PS-64-QAM symbols, in which 3072 symbols are used as the preamble. After up-sampling, the sequence is

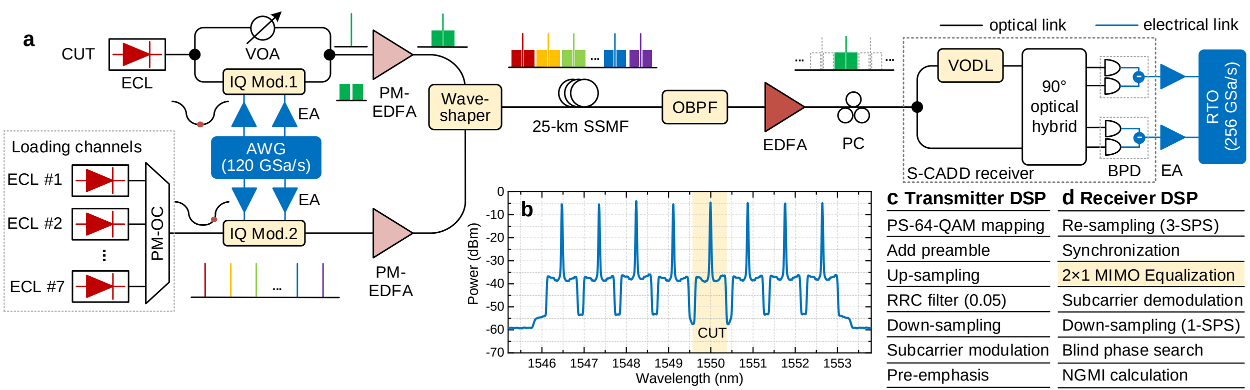

Fig. 2. (a) Experimental setup. CUT: channel under test; ECL: external cavity laser; IQ Mod.: IQ modulator; AWG: arbitrary waveform generator; EA: electrical amplifier; PM-EDFA: polarization-maintaining erbium-doped fiber amplifier; SSMF: standard single-mode fiber; OBPF: optical band-pass filter; PC: polarization controller; VODL: variable optical delay line; BPD: balanced photodiode; RTO: real-time oscilloscope. (b) Measured optical spectrum of 8-channel WDM signals after the wave-shaper. (c) Transmitter- and (d) receiver-side DSP stacks. PS: probabilistic shaped; RRC: root-raised cosine; MIMO: multi-input-multi-output; SPS: sample-per-symbol.

Nyquist-shaped with 0.05 roll-off. The waveform is down-sampled to match the AWG sampling rate. We reserve a 3 GHz guard band around the zero-frequency, and the two 42-GBd subcarriers are up-converted and combined. We apply a linear digital pre-emphasis to compensate for the frequency response of AWG, EA, and IQ modulators. At the receiver, we first re-sample the waveform to 3 samples-per-symbol to avoid spectral overlap. After synchronization, a 121-tap real-valued 2×1 MIMO equalizer is adopted for optical field recovery. The tap coefficients are updated by the recursive least square (RLS) algorithm based on the preamble. For SSBI-C, we further use 65 2^{nd}-order and 9 3^{rd}-order diagonal-only kernels. Due to the residual optical path mismatch at the transmitter, we apply blind phase search algorithm to rotate the symbols, which can be avoided in self-coherent detection. Finally, normalized generalized mutual information (NGMI) is calculated to indicate the performance. We choose a NGMI threshold of 0.857, which is supported by a concatenated FEC with a total code rate R_c of 0.826 [12].

4. Experimental results and discussion

We first optimize the CSPR after 25-km SSMF transmission. As depicted in Fig. 3(a), the NGMI increases with CSPR and gets saturated at 19 dB. By comparing the curves with and without SSBI-C, larger NGMI improvement is obtained at the low-CSPR region, which is dominated by SSBI impairment. Note that the 19-dB CSPR is comparable with intensity-modulated PAM-*n* signals, and there is a sufficient optical signal-to-noise ratio (OSNR) in short-reach scenarios. Then we sweep the source entropy in Fig. 3(b) and 3(c) to maximize the bitrate. At the NGMI threshold of 0.857, entropies of 5.75 bits/symbol and 5.5 bits/symbol can be supported at BTB and 25-km SSMF, respectively. The corresponding single-channel line rate is 483 Gb/s and 462 Gb/s. After excluding the FEC overhead, the net data rates are calculated as 395.3 Gb/s and 374.3 Gb/s. We also observe that the NGMI penalty at 25 km SSMF increases with the source entropy. It can be attributed to the enhanced peak-to-average power ratio (PAPR) after fiber dispersion, and the SSBI cannot be fully mitigated under the insufficient CSPR. Moreover, the received optical power (ROP) sensitivity is measured in Fig. 3(d) and 3(e). With the help of SSBI-C, ~2.5 dB and 4.2 dB improvement in ROP sensitivity can be obtained, respectively. Finally, we measured the NGMI versus channel index in an 8-channel WDM transmission case. Here the channels are labeled from long to short wavelengths. By using SSBI-C, all 8 channels can achieve the NGMI threshold. The average generalized mutual information (GMI) gain is 0.14 bits/symbol compared with linear equalization only.

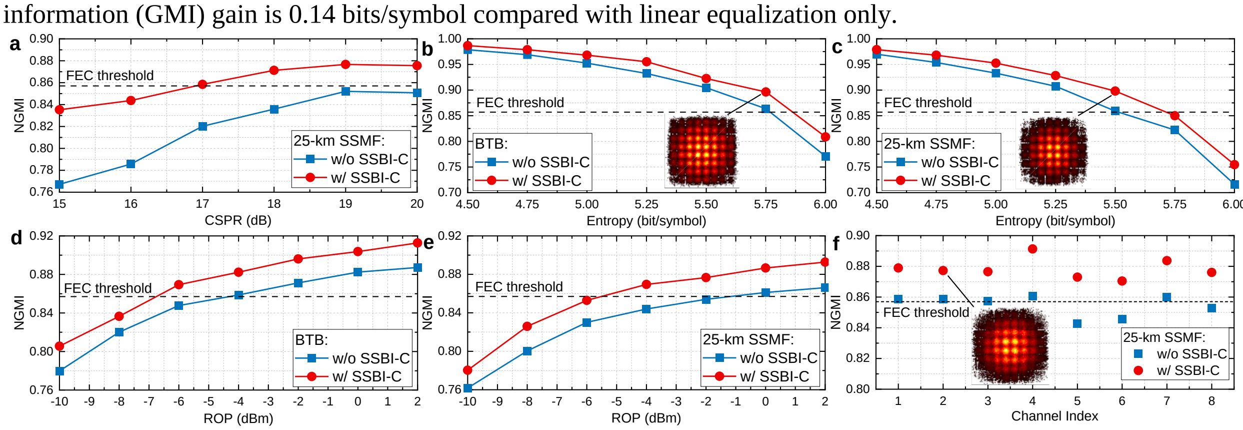

Fig. 3. (a) Measured NGMI versus CSPR at 25-km SSMF with and without SSBI cancellation. Measured NGMI versus source entropy at (b) back-to-back (BTB) and (c) 25-km SSMF, respectively. Measured NGMI versus received optical power at (d) back-to-back and (e) 25-km SSMF, respectively. (f) Measured NGMI versus channel index in 8-channel WDM at 25-km SSMF. w/o: without; w/: with.

4. Conclusions

In summary, we experimentally demonstrate 8-channel WDM transmission of 462-Gb/s PS-64-QAM signals with direct detection based on the hardware-efficient symmetric CADD receiver and delay-unknown field recovery. The gross capacity is 3.70 Tb/s and the net capacity is 2.99 Tb/s. To our best knowledge, we achieve the highest E-SE of 8.3 b/s/Hz among single-polarization direct detection receivers, which is comparable with intradyne coherent receivers. The proposed scheme offers a spectrally efficient solution for the future 3.2Tb-class DCI campus scenario.

Acknowledgments

This work is supported by National Key R&D Program of China (2022YFB2903500), and National Natural Science Foundation of China (62271305, 62001287).

References

[1] X. Zhou, *et al.*, *J. Lightw. Technol.*, **38**(2), 475-484 (2019).
[2] K. Kikuchi, *et al.*, *J. Lightw. Technol.*, **34**(1), 157-179 (2016).
[3] Md M. H. Adib, *et al.*, in Proc. OFC'2019, paper Th3F.4.
[4] D. Che, *et al.*, *J. Lightw. Technol.*, **34**(2), 516-524 (2016).
[5] A. Mecozzi, *et al.*, *Optica*, **3**(11), 1220-1227 (2016).
[6] H. Chen, *et al.*, *J. Lightw. Technol.*, **38**(9), 2587-2597 (2020).
[7] W. Shieh, *et al.*, *Light: Sci. Appl.*, **9**(1), 1-9 (2020).
[8] X. Li, *et al.*, *Opt. Express*, **29**(16), 25412-25427 (2021).
[9] H. Chen, *et al.*, in Proc. OFC'2021, paper Th4D.3.
[10] Y. Zhu, *et al.*, *Opt. Express*, **28**(13), 19008-19022 (2020).
[11] J. R. Fienup, *Appl. Opt.*, **21**(15), 2758–2769 (1982).
[12] H. Yamazaki, *et al.*, *Opt. Express*, **27**(18), 25544-25550 (2019).